34th Annual International Conference of the IEEE EMBS
San Diego, California USA, 28 August - 1 September, 2012

# Extraction of Control Signals from a Mixture of Source Activity in the Peripheral Nerve

Y. Tang, B. Wodlinger, and D.M. Durand, *Member, IEEE*

***Abstract*— Extracting physiological signals to control external devices such as prosthetics is a field of research that offers great hope for patients suffering from disabilities. In this paper, we present an algorithm for isolating control signals from peripheral nerve cuff recordings. The algorithm is able to extract individual control signals from a mixture of source signal activity while maximizing SNR and minimizing cross-talk between the control signals. Based on fast independent component analysis *FICA* and an adaptation of *Champagne*, the proposed algorithm is tested against previously published results obtained using beamforming techniques in an acute preparation of rabbits. Preliminary results demonstrate an improvement in performance.**

## I. INTRODUCTION

Research into the extraction of physiological source signals from human subjects to control external devices offers numerous possibilities to improve the lives of disabled patients. In this paper, we develop an algorithm to extract control signals from the peripheral nerve using the Flat Interface Nerve Electrode (FINE). Peripheral nerve activities offer several advantages over brain signals: (a) the functional anatomy of the peripheral nerves are known and is considerably more structured and simpler. This can lead to less interferences and more stable source signals. (b) The physiological functions of the individual nerves are known facilitating the generation of controlled signals by human subjects. (c) The implant procedures are less invasive compared to ECoG. The extraction of viable control signals from the peripheral nerve is a challenging task that requires the isolation of individual sources from recordings that consist of a mixture of source activity contaminated with noise and interference. In this paper, we present a control signal extraction algorithm using fast independent component analysis *FICA* [2] as well as an adaptation of *Champagne* [3, 4]. The algorithm is designed to isolate potential control signals from a mixture of peripheral nerve source activity while both maximizing the SNR of the extracted control signals and minimizing the crosstalk interference between them.

This work was sponsored by the Defense Advanced Research Projects Agency (DARPA) MTO under the auspices of Dr. Jack Judy through the Space and Naval Warfare Systems Center, Pacific Grant/Contract No. N66001-12-C-4173

Y. Tang is with the Department of Biomedical Engineering, Case Western Reserve University, Cleveland, OH 44106 USA (phone:405-503-9920; fax: 216-368-4872; e-mail: dyt1@ case.edu).

B. Wodlinger was with the Department of Biomedical Engineering, Case Western Reserve University, Cleveland, OH 44106 USA. He is now with the Department of Physical Medicine and Rehabilitation, University of Pittsburgh, Pittsburgh, PA 15260 USA (e-mail: bcw12@case.edu).

D.M. Durand is with the Department of Biomedical Engineering, Case Western Reserve University, Cleveland, OH 44106 USA (email: dxd6@ case.edu).

## II. METHODS

Given a segment of recorded nerve activity $\boldsymbol{Y}^{KxN}$, where $N$ is the number of time points and $K$ is the number of electrode contacts, it is our objective to learn a set of spatial filters $\boldsymbol{F}_j^{1xK}$ that can each extract a corresponding control signal $\boldsymbol{X_j}$ from the recorded signals $\boldsymbol{Y}$.

$$\boldsymbol{X}_j = \boldsymbol{F}_j\boldsymbol{Y} \tag{1}$$

### *A. Data Collection*

In this section, methods for acquiring $\boldsymbol{Y}$ are described. New Zealand White Rabbits are anesthetized with 20-50 mg/kg IM ketamine and 5 mg/kg IV diazepam and maintained with 60 mg/kg IV alpha-chloralose (followed by one quarter dose every 2 hours or as needed) and .02 mg/kg IM buprenex. All protocols are approved by the Case Western Reserve University IACUC. Recordings are made from a novel 16-channel tripolar FINE placed on the sciatic trunk near the popliteal fossa. The FINE offers improved recording selectivity by reshaping the geometry of the nerve [5, 6]. The signals are AC coupled, amplified, multiplexed and low-pass filtered at 5 kHz by an RHA1016 preamplifier chip (Intan Technologies, Utah). A National Intruments data acquisition card is used to perform A-to-D conversion and sampling at 15 kHz/channel. Tripolar stimulating FINEs are placed on the Tibial and Peroneal branches of the Sciatic nerve, distal to the recording cuff. 5kHz sinusoidal electrical stimulations are applied to each individual nerve branch separately as well as together to generate pseudo-spontaneous source activities [7] where the Peroneal/Tibial activity each present a potential control signal, $D_X$ = 2. Recorded signals are post-processed using an 800Hz – 3 kHz band-pass filter in order to reduce any non-essential EMG and stimulation artifacts.

### *B. Spatial Filter Construction and Validation*

During training, it is unlikely that individual sources within a peripheral nerve can be activated separately. Instead, the spatial filters $\boldsymbol{F}$ must be learned from signals containing a mixture of source activity. Therefore, in this study, the spatial filters $\boldsymbol{F}$ are built only from data obtained where the Tibial and Peroneal branches are both activated simultaneously. Segments of the data where the Tibial and Peroneal branches are activated individually are only used to quantify the quality of the resulting spatial filters $\boldsymbol{F}_j$ using the SNR defined as

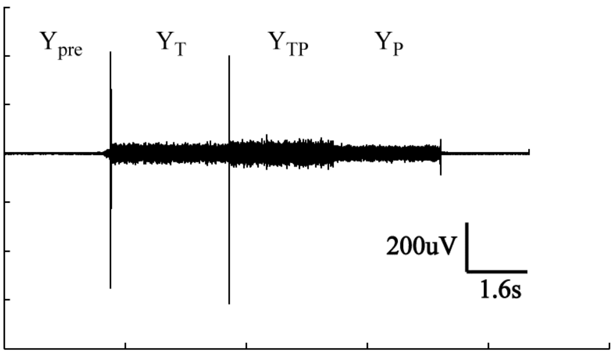


Figure 1. Illustration of the recorded peripheral nerve activity. The average signal from the 16 contacts is plotted. $\boldsymbol{Y_{pre}}$ is the background activity, $\boldsymbol{Y_T}$ is period of Tibial stimulation, $\boldsymbol{Y_{TP}}$ is period of Tibial and Peroneal stimulation and $\boldsymbol{Y_P}$ is period when only Peroneal stimulation occurs.

$$\text{SNR}(\boldsymbol{F}_j) = 10\log(\text{P}(\boldsymbol{X}_j)/\text{P}_{\text{background}}) \quad (2)$$

as well as the cross-talk ratio CTR defined as

$$\text{CTR}(\boldsymbol{F}_j) = 10\log(\text{P}(\boldsymbol{X}_j)/\text{P}(\boldsymbol{X}_{i\neq j})) \quad (3)$$

where P is power.

Given data recording $\boldsymbol{Y}$ consisting of four separate periods in the following order, $\boldsymbol{Y_T}$, $\boldsymbol{Y_{TP}}$ and $\boldsymbol{Y_P}$ shown in Fig. 1, we first follow the methods described in [3] to de-noise $\boldsymbol{Y_{TP}}$ to yield $\boldsymbol{Y_{TPDe}}$ using only the information in $\boldsymbol{Y_{pre}}$ and $\boldsymbol{Y_{TP}}$. The nerve recordings $\boldsymbol{Y_{TP}}$ are modeled as a combination of source signals $\boldsymbol{S}$ interference signals $\boldsymbol{U}$ and random noise $\boldsymbol{V}$.

$$\boldsymbol{Y} = \boldsymbol{AS} + \boldsymbol{BU} + \boldsymbol{V} \quad (4)$$

The source and interference signals are assumed to be independent Gaussian distributions with zero mean and unit precision. The random noise term $\boldsymbol{V}$ is described by a diagonal precision matrix $\boldsymbol{C_V}$. Given an initial choice of the number of sources and interferences to be learned, the algorithm utilizes variational Bayes expectation maximization to learn the set of model parameters that best fit the data covariance matrix $\boldsymbol{C_Y}$ by

$$\boldsymbol{C_Y} \approx \boldsymbol{AA^T} + \boldsymbol{BB^T} + \boldsymbol{C_V} \quad (5)$$

using $\boldsymbol{Y_{pre}}$ to first learn the interference and noise parameters $\boldsymbol{B}$ and $\boldsymbol{C_V}$ then fixing these parameters while learning the remaining parameters using $\boldsymbol{Y_{TP}}$ with $\boldsymbol{Y_{TPDe}} = \boldsymbol{AX}$ as a denoised version of $\boldsymbol{Y_{TP}}$.

During the next step, *FICA* is used to decompose $\boldsymbol{Y_{TPDe}}$ into $K$ number of independent components $\boldsymbol{IC}_{j=1:K}$ such that

$$\boldsymbol{Y_{TPDe}} = \boldsymbol{WIC} \quad (6)$$

where $\boldsymbol{W}$ is the mixing matrix. It is our hypothesis that some of the $\boldsymbol{IC_j}$ will represent individual source activity $\boldsymbol{S}_\text{j}$ where it's either Tibial or Peroneal and that different $\boldsymbol{IC_j}$ composed mostly of the same source activity will have similar spatial distributions. With this in mind, spatial filters $\boldsymbol{FIC}_j$ are constructed for each individual $\boldsymbol{W}_j\boldsymbol{IC}_j$ using *Champagne [4]*. The Pearson's correlation coefficient R is then computed between each pair of ($\boldsymbol{FIC}_j$ and $\boldsymbol{FIC}_{i\neq j}$). For the pair that yielded the highest R value, the components are combined together $\boldsymbol{W}_{j,i}\boldsymbol{IC}_{j,i}$ and a new $\boldsymbol{FIC}_{j+i}$ is learned. This process is iterated until a minimum correlation threshold is reached. The final $\boldsymbol{FIC}_j$ with minimum correlation between each other can then be considered as good candidates for extracting useful control signals.

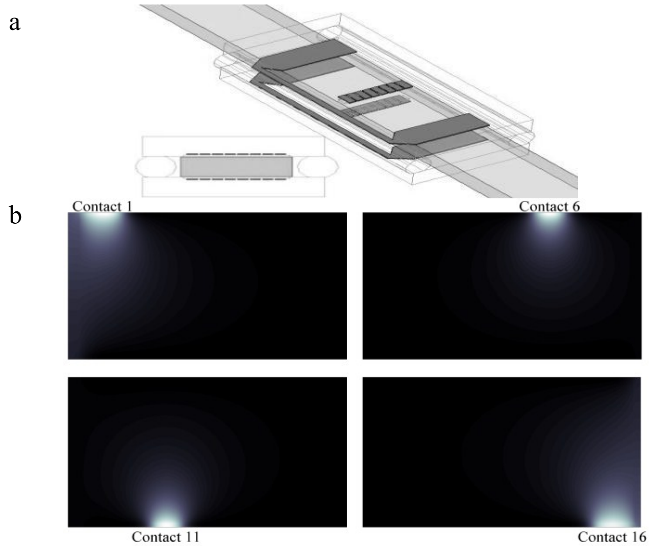


Figure 2. (a) The finite element model of the FINE electrode measuring 5mm by 1.5mm and divided into 82 by 208 pixels [1]. (b) The pixel-sensitivity described by the lead field matrix L for electrodes 1, 6, 11 and 16.

In constructing spatial filters to extract control signals, each spatial filter not only have to isolate the control signal it is responsible for from both background noise and interference, it must also be able to reject the activity from other source signals which also act as interferences for the current control signal of interest. To accomplish this, we have developed an adaptation of the *Champagne* algorithm. Briefly *Champagne* is a source localization algorithm that models $\boldsymbol{Y}$ as

$$\boldsymbol{Y} = \boldsymbol{LS}_{pix} + \boldsymbol{e} \quad (7)$$

where $\boldsymbol{S}_{pix}$ is a $M$ by $N$ matrix. $M$ is the number of pixels within the cross section of the FINE finite element model. Each pixel is a potential source that have influences on the $K$ FINE contacts described by the lead field matrix $\boldsymbol{L}^{KxM}$ . The various noise and interference that exist within the system are described by $\boldsymbol{e}$. Detailed explanation of the lead field matrix $\boldsymbol{L}$ can be found in [1]. In short, a rectangular finite element model of the FINE positioned over an empty epineurium enclosing a homogeneous volume conductor is created, Fig. 2a.

The FINE, measuring 5mm by 1.5mm, consists of 16 contacts with contacts 1 to 8 arranged from top left to top right and contacts 9 to 16 from bottom left to bottom right. The cross section of the FINE is divided into 82 by 208 pixels, which leads to $M$ = 17056. In Fig. 2b, the sensitivities of the four contacts (1, 6, 11 and 16) to the M pixels are plotted.

To estimate the source locations *Champagne* introduces the following likelihood model based on (7)

$$p(\boldsymbol{Y}|\boldsymbol{S}) \propto exp(-0.5 \| \boldsymbol{Y} - \boldsymbol{LS_{pix}} \|^2_{Ce}) \quad (8)$$

where $\| Q \|_C = (\mathrm{trace}[Q^T C^{-1} Q])^{1/2}$ and

$$\boldsymbol{C_e} = \boldsymbol{BB^T} + \boldsymbol{C_V}. \quad (9)$$

The sources $\boldsymbol{S_{pix}}$ are modeled as independent zero mean Gaussian distributions with covariance $C_{Spixi}$ for each pixel $\boldsymbol{S_{pixi}}$. The approximation of $\boldsymbol{C_S}$ infers the pixel locations where the sources most likely reside. When this approximation is complete, spatial filters $\boldsymbol{F}$ can be constructed as

$$\boldsymbol{F} = \boldsymbol{C_S L}^T(\boldsymbol{C_e} + \boldsymbol{LC_S L}^T)^{-1}. \quad (10)$$

To learn $\boldsymbol{C_S}$ we minimize the following cost function

$$\boldsymbol{L(C_S)} = \mathrm{trace}[\boldsymbol{C_Y C_E^{-1}}] + \log(|\boldsymbol{C_E}|) \quad (11)$$

where $\boldsymbol{C_E} = \boldsymbol{C_e} + \boldsymbol{LC_S L}^T$ and $\boldsymbol{C_Y} = \boldsymbol{YY}^T/dt$. In order to construct spatial filters that minimize cross-talk interference between control signals we propose to modify (8) to

$$\boldsymbol{C_e} = \boldsymbol{BB^T} + \boldsymbol{C_V} + \boldsymbol{C_{int}} \quad (12)$$

where $\boldsymbol{C_{int}}$ measures the covariance of the interfering source signals. In this study, the mixing matrix $\boldsymbol{W}$ for the final $\boldsymbol{IC}$ can be used such that $\boldsymbol{C_{int}} = \boldsymbol{WW}^T$. For $\boldsymbol{W}$ to be accurate, each $\boldsymbol{IC_j}$ should be normalized to have unit variance.

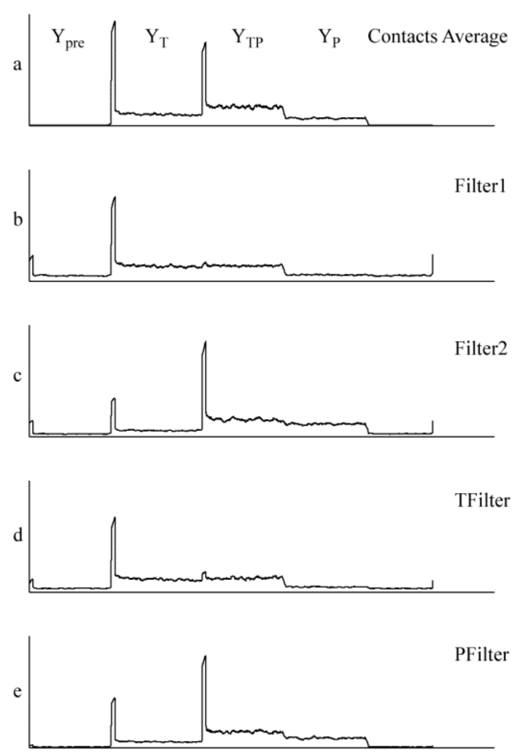


Figure 3. (a)Average power across the 16 contacts. (b) Power of Filter1 output which extracts the Tibial activity. (c) Power of Filter2 output which extracts Peroneal activity. (d) Power output from Tibial filter constructed from [1]. (e) Power output from Peroneal filter constructed from [1].

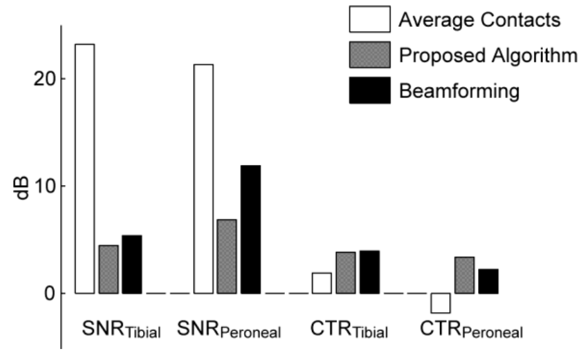


Figure 4. SNR and CTR comparison between the average contacts signal, the output signal obtained from the proposed algorithm and the output signal obtained from the filters constructed in [1].

## III. RESULTS

Fig. 3 illustrates the implementation of the algorithm. Filter1 and Filter2 are constructed using the methods detailed above. The original recording is then filtered through each filter and the results plotted. In Fig. 3a, 130 ms running power average is plotted for the average signal recorded across the 16 contacts. Fig. 3b and 3c plots the output of Filter1 and Filter2 separately. From the results, it is clear that Filter1 extracts the Tibial activity and rejects the Peroneal activity while Filter2 extracts the Peroneal activity with some crosstalk from Tibial activity. Fig. 3d and 3e are the power outputs of the Tibial and Peroneal filter constructed in [1]. While these filters also perform very well, they are constructed from activating each individual nerve branch separately using 130Hz stimulation that generates strong periodic compound action potentials that are then time averaged to eliminate noise. This is an ideal signal that cannot be duplicated in realistic environments. In Fig 4., the SNR and CTR are compared between averaging the signals across each contact, the output of Filter1 and Filter2 obtained from the proposed algorithm and PFilter/TFilter obtained from the beamforming strategy in [1]. It can be observed from the figure that the highest SNR is obtained from simply averaging the contacts together. However signals obtained with this method are useless due to crosstalk interference across the sources. On the other hand, both [Filter1, Filter2] and [PFilter, TFilter] have reduced SNR but with significantly better CTR. Since either a low SNR or CTR will negatively impact the utility of the extracted control signals, a balance between SNR and CTR offers the best performance.

## IV. CONCLUSION

In this paper, we proposed a novel source signal extraction method based on the Bayesian algorithm *Champagne* and FICA. The algorithm is able to extract control signals from a mixture of recorded source activity while maximizing the SNR and minimizing the crosstalk between sources. Currently statistical significance cannot be computed due to the preliminary nature of the data. Future work will include further trials using the proposed algorithm.

## ACKNOWLEDGMENT

Y.T. author thanks Dr. Sri Nagarajan for his help with *Champagne*.


## REFERENCES


1. Wodlinger, B. and D.M. Durand, *Localization and Recovery of Peripheral Neural Sources With Beamforming Algorithms.* Neural Systems and Rehabilitation Engineering, IEEE Transactions on, 2009. **17**(5): p. 461-468.
2. Hyvarinen, A., *Fast and robust fixed-point algorithms for independent component analysis.* IEEE Trans Neural Netw, 1999. **10**(3): p. 626-34.
3. Nagarajan, S.S., et al., *A probabilistic algorithm for robust interference suppression in bioelectromagnetic sensor data.* Statistics in medicine, 2007. **26**(21): p. 3886-910.
4. Wipf, D.P., et al., *Robust Bayesian estimation of the location, orientation, and time course of multiple correlated neural sources using MEG.* NeuroImage, 2010. **49**(1): p. 641-55.
5. Durand, D.M., P. Yoo, and Z. Lertmanorat. *Neural interfacing with the peripheral nervous system*. in *Engineering in Medicine and Biology Society, 2004. IEMBS '04. 26th Annual International Conference of the IEEE*. 2004.
6. Yoo, P.B. and D.M. Durand. *The recording properties of a multi-contact nerve electrode as predicted by a finite element model of the canine hypoglossal nerve*. in *Engineering in Medicine and Biology Society, 2004. IEMBS '04. 26th Annual International Conference of the IEEE*. 2004.
7. Rubinstein, J.T., et al., *Pseudospontaneous activity: stochastic independence of auditory nerve fibers with electrical stimulation.* Hear Res, 1999. **127**(1-2): p. 108-18.